AC NEGF Simulation of Nanosheet MOSFETs

Sung-Min Hong and Phil-Hun Ahn
School of EECS, Gwangju Institute of Science and Technology, Gwangju, Republic of Korea, email: smhong@gist.ac.kr

***Abstract*—In this work, an AC nonequilibrium Green function (NEGF) simulation for nanosheet MOSFETs is presented. The AC NEGF equations are discretized using a decoupled mode-space approach for efficient implementation. The Poisson equation is solved self consistently to obtain the electrostatic potential. Our in-house device simulator, G-Device, is used to simulate the AC responses on nanosheet MOSFETs.**

I. Introduction

During the last couple of decades, the NEGF (Nonequilibrium Green's function) formalism [1], [2], [3] has become the $defacto$ standard method for the quantum transport modeling. It has been actively applied to the simulation of nanoscale transistors.

However, in most cases, the NEGF technique has been applied only to the DC (steady-state) simulation. It is difficult to find transient and AC simulation results for semiconductor devices. In contrast, TCAD tools are fully capable of DC, transient, and AC simulation. These days, even the BTE (Boltzmann transport equation) solvers [4], [5], [6], [7] can solve the transient Boltzmann equation.

Although recent theoretical advances have extended the method to the AC (small-signal) simulation [8], [9], it is difficult to find the AC NEGF simulation results of the electronic devices. It is expected that the frequency-domain analysis, which is fully consistent with the DC NEGF technique, can expand a new horizon of the quantum transport modeling. For example, the maximum limit of the intrinsic RF performance in the nanoscale MOSFET can be investigated by this analysis. Understanding the intrinsic limit of the RF performance is critically important to realize the terahertz (THz) electronics based on the MOSFET technology.

In this work, the AC NEGF code is implemented. Based upon the solution of the conventional DC NEGF simulation, the AC response to the voltage excitation with a given frequency is calculated by adopting the quantum transport theory. The AC response of the nanosheet MOSFET is evaluated. In Section II, the AC NEGF formalism is briefly explained. In Section III, the implementation of the AC NEGF formalism is discussed. A robust method to get the AC electrostatic potential is discussed. The simulation results for the nanosheet MOSFET are presented in Section IV. Finally, the conclusion is made in Section V.

II. Methodology

Detailed derivation procedure of the AC NEGF formalism can be found in [8], [9]. Only some important relations in [8] are selectively introduced below.

When the AC voltage excitation, whose amplitude and angular frequency are v_{amp} and ω, respectively, is applied to a contact, the retarded Green function is written as a sum of the DC retarded Green function and the AC one,

$$G^r(E) = G^r_{DC}(E) + G^r_{AC}(E), \tag{1}$$

where E is the energy. It is noted that those quantities are matrices representing their position dependence, $\mathbf{r}$ and $\mathbf{r}'$. Here, the AC retarded Green function, $G^r_{AC}(E)$, is given by

$$G^r_{AC}(E) = \\ G^r_{DC}(E+\hbar\omega)\left[V_{AC} + \Sigma^r_{AC}(E+\hbar\omega, E)\right] G^r_{DC}(E), \tag{2}$$

where $\hbar$ is the reduced Planck constant, $V_{AC}(\omega)$ is the AC potential energy determined by the Poisson equation, and $\Sigma^r_{AC}(E+\hbar\omega, E)$ is the AC retarded self-energy. The AC retarded self-energy due to the voltage excitation at a contact is given by

$$\Sigma^r_{AC}(E+\hbar\omega, E) = -\frac{q v_{amp}}{\hbar\omega}\left[\Sigma^r_{DC}(E) - \Sigma^r_{DC}(E+\hbar\omega)\right], \tag{3}$$

where q is the absolute elementary charge.

Once the AC retarded Green function is obtained, the AC lesser Green function, $G^<_{AC}(E)$, is calculated. It is given by

$$\begin{aligned} G^<_{AC}(E) = {} & G^r_{DC}(E+\hbar\omega)\Sigma^<_{DC}(E+\hbar\omega)G^r_{AC}(E)^\dagger \\ & + G^r_{DC}(E+\hbar\omega)\Sigma^<_{AC}(E)G^r_{DC}(E)^\dagger \\ & + G^r_{AC}(E+\hbar\omega)\Sigma^<_{DC}(E)G^r_{DC}(E)^\dagger, \end{aligned} \tag{4}$$

where the AC lesser self-energy is also written as

$$\Sigma^<_{AC}(E) = -\frac{q v_{amp}}{\hbar\omega}\left[\Sigma^<_{DC}(E) - \Sigma^<_{DC}(E+\hbar\omega)\right]. \tag{5}$$

From the AC lesser Green function, the AC response of the electron density, $n_{AC}(\mathbf{r})$, can be easily obtained by an integration,

$$n_{AC}(\mathbf{r}) = -i\int \frac{dE}{2\pi} G^<_{AC}(\mathbf{r}, \mathbf{r}, E). \tag{6}$$

As much as the contact self-energy is concerned, according to (3) and (5), the AC self-energies can be easily calculated from the DC ones. The DC retarded self-energy at the source (or drain) terminal is obtained by assuming the semi-infinite leads. [10] Also the DC lesser self-energy defined at the source terminal can be written as:

$$\Sigma^{<,S}_{DC}(E) = i(-2)\,\mathrm{Im}\left\{\Sigma^{r,S}_{DC}(E)\right\} f^s(E), \tag{7}$$

where $f^s(E)$ is the Fermi-Dirac function evaluated at the source terminal. The expressions for the drain terminal are similar and not repeated here.

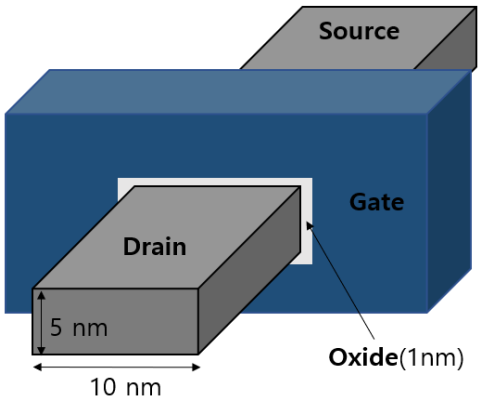

Fig. 1. Silicon nanosheet MOSFET with 5 nm × 10 nm cross section, 1 nm oxide thickness, and 7 nm channel length.

A decoupled mode-space approach is used for an efficient implementation. Using this approach, real and imaginary parts are separated and obtained consistently with the mode-space approach. The size of the matrix is determined by the number of modes multiplied with the number of 1D real space grid points. The AC NEGF solver has been implemented in our in-house device simulator, G-Device. It was previously applied to the THz simulation [11] and the transient BTE simulation [12].

III. Numerical Results

In order to demonstrate the AC NEGF simulation, a silicon nanosheet transistor with 5 nm × 10 nm cross section, 1 nm oxide thickness, and 7 nm channel length is simulated, as illustrated in Fig. 1. A uniform yz cross section is assumed. The entire length of structure is 25 nm. Source/drain regions are 9-nm-long and the doping density is 10^{20} cm^{-3}, while the channel region is intrinsic. The gate contact is 7-nm-long and its workfunction is 4.3 eV. The effective mass Hamiltonian is employed to describe six elliptical valleys in the silicon conduction band. In addition, (001) surface and [100] channel are assumed. V_{DD} is set to be 0.5 V.

Before the AC NEGF simulation, the DC NEGF simulation is performed. Five lowest modes in each valley pair are considered in the simulation. An energy range of (-0.6 eV, 0.6 eV) is adopted. The ballistic transport is assumed. The self-consistent solution of the NEGF-Poisson system is obtained by using a conventional Gummel loop. The convergence criterion of the DC NEGF simulation is the potential error smaller than 10^{-5} times the thermal voltage. The five lowest mode energies for each valley pair is shown in Fig. 2. Since the z-directional length of the silicon channel (5 nm) is much smaller than the y-directional one (10 nm), the [001] valley whose z-directional mass is heavy has the lowest mode energy.

The DC input current-voltage curve of the transistor is shown in Fig. 3. The threshold voltage is about 0.23 V. The DC output current-voltage curve of the transistor is shown in Fig. 4. The ON current at $V_{GS} = V_{DC} = V_{DD}$ is about 50 μA. It is noted that curves in Figs. 3 and 4 are obtained

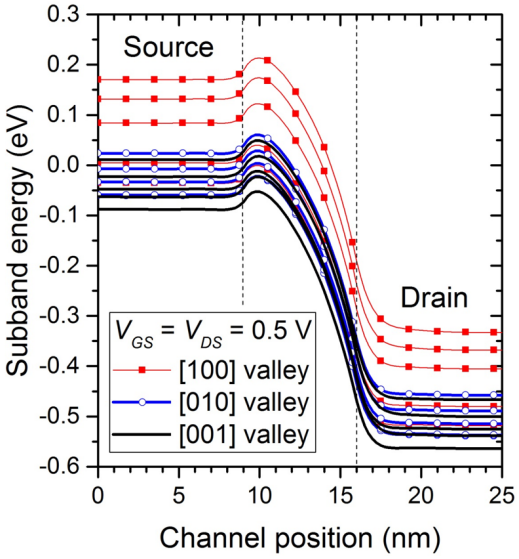

Fig. 2. Five lowest mode energies along the channel direction. Three elliptical valley pairs are considered.

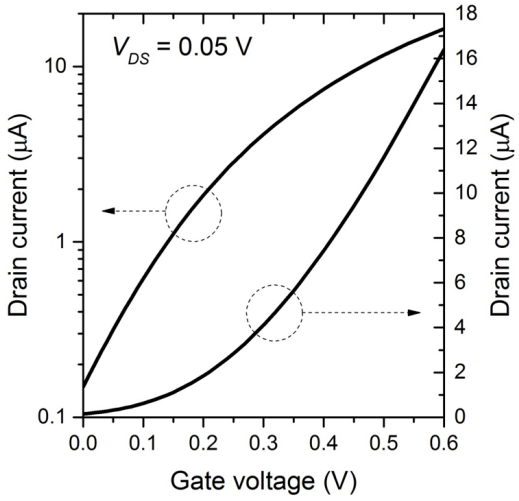

Fig. 3. DC I_D-V_G curve of the nanosheet transistor. V_{DS} = 0.05 V.

from the bias ramping procedure. The converged solution at the previous bias point is used as an initial solution of the Gummel loop.

When we recall (2) and (4), we need quantities like $G^r_{DC}(E+\hbar\omega)$, $G^r_{DC}(E)$, $G^<_{DC}(E+\hbar\omega)$, $G^<_{DC}(E)$, and so on. Therefore, the minimum frequency used in the AC NEGF simulation is determined by the energy spacing adopted in the DC NEGF simulation. For example, when the energy spacing of 0.2 meV corresponds to about 48 GHz. When we want to calculate the AC response at 0.2 THz, the maximum allowed energy spacing is 0.827 meV. In order to calculate the AC response at a very low frequency, a very fine energy grid should be introduced.

However, at the low frequency limit, such restriction can be relaxed. AC self-energies in (3) and (5) can be approximated

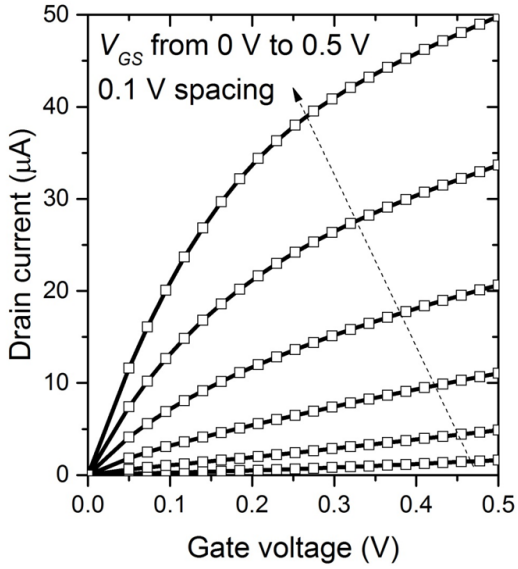

Fig. 4. DC I_D-V_D curve of the nanosheet transistor. Various V_{GS} values are considered.

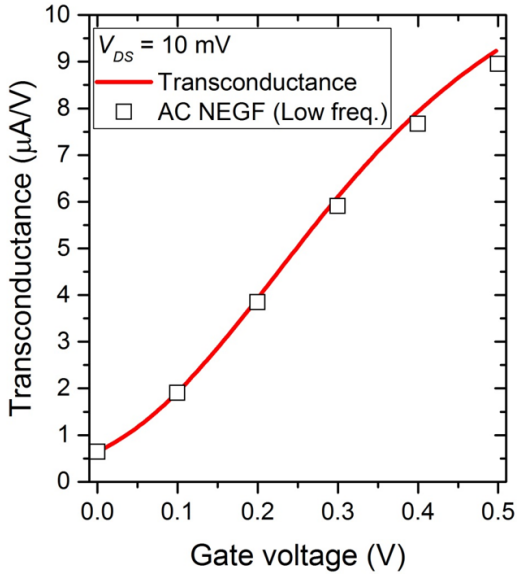

Fig. 5. Transconductance of the nanosheet transistor at the low frequency limit. Square symbols are results of the AC NEGF simulation. V_{DS} = 10 mV.

as

$$\lim_{\omega\to 0}\Sigma^r_{AC}(E+\hbar\omega,E)=qv_{amp}\frac{\partial\Sigma^r_{DC}}{\partial E}, \tag{8}$$

$$\lim_{\omega\to 0}\Sigma^<_{AC}(E+\hbar\omega,E)=qv_{amp}\frac{\partial\Sigma^<_{DC}}{\partial E}, \tag{9}$$

respectively. AC Green functions in (2) and (4) can be easily evaluated with the AC self-energies, $G^r_{DC}(E)$, and $G^<_{DC}(E)$.

At the low frequency limit, the admittance, $Y_{DG}(\omega)$, must converge to the transconductance. In Fig. 5, the transconductance of the nanosheet transistor, which is calculated from the DC simulation results with the finite difference, is shown. The low frequency admittance from the AC NEGF simulation shows a good agreement. Similarly, $Y_{DD}(\omega)$ at the low frequency limit should be an inverse of the output resistance. In Fig. 6, the output resistance of the nanosheet transistor is shown. Again, the AC NEGF simulation results show good agreement with the quasi-static results. In addition to the terminal currents, internal quantities such as the electron density should be checked. Electron density integrated over the yz-plane for a gate excitation or a drain excitation is shown in Fig. 7.

At nonzero frequencies, the wideband limit approximation is used for contacts, only because it greatly simplifies the implementation. A slightly modified version of the structure shown in Fig. 1 (long source/drain regions) is simulated. An isotropic effective mass is considered and only the lowest mode is calculated.

The AC total current is obtained by summing the particle current and the displacement current [8]. The frequency dependence of $Y_{GG}(\omega)$ is shown in Fig. 8. The real and imaginary parts are illustrated separately. $Y_{DG}(\omega)$ is also shown in Fig. 9. Its real part rapidly decreases at high frequencies. It is noted that the minimum frequency (48 GHz) is related with the

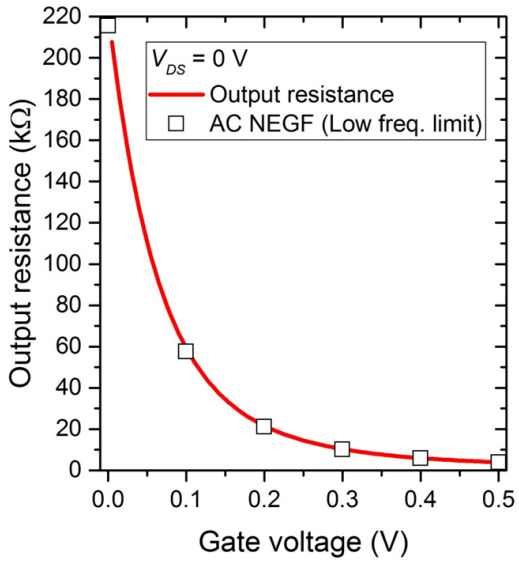

Fig. 6. Output resistance of the nanosheet transistor at the low frequency limit. Square symbols are results of the AC NEGF simulation. V_{DS} = 0 V.

energy spacing used in the DC NEGF simulation, as explained already.

IV. Conclusion

In summary, the AC NEGF simulation approach has been demonstrated for nanosheet MOSFETs. At the low frequency limit, the AC NEGF simulation results have been compared with the quasi-static results. AC terminal currents at nonzero frequencies have been evaluated under the wideband limit approximation. The result represents that the nanoscale device exhibits complicated frequency dependence on the external voltage excitation.

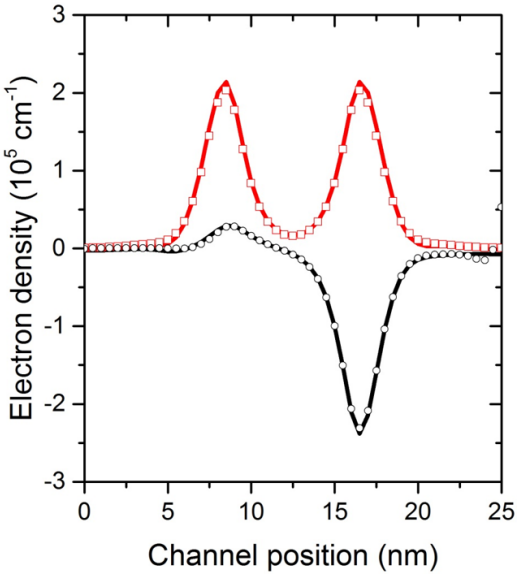

Fig. 7. Integrated electron density for a gate excitation (Red line) or a drain excitation (Black line) along the channel position. For the DC NEGF simulation, V_{GS} = V_{DS} = 0.0 V. The amplitude of a voltage excitation is 5 mV. Symbols represent the AC NEGF simulation results.

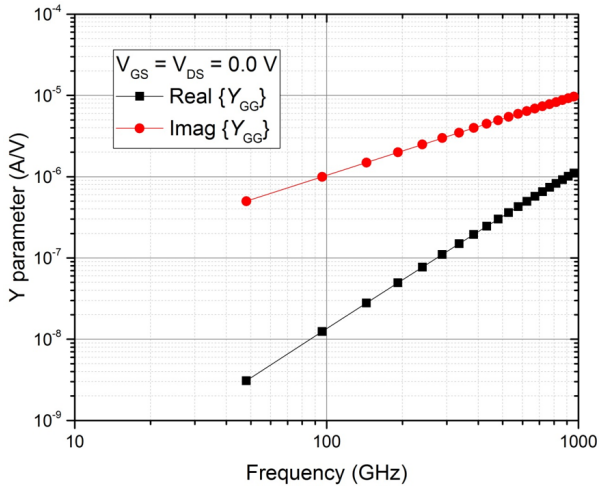

Fig. 8. $Y_{GG}(\omega)$ of the nanosheet transistor. The frequency varies from 48 GHz to 1 THz. V_{GS} = V_{DS} = 0.0 V. The wideband limit approximation is applied.

As a future work, the AC NEGF simulation will be extended to more general cases beyond the wideband limit approximation and the ballistic transport. Additionally, the proof of the current conservation under the conventional simulation set up would be an interesting future research topic.

Acknowledgement

This work was supported by the National Research Foundation of Korea (NRF) grant funded by the Korea government (NRF-2019R1A2C1086656).

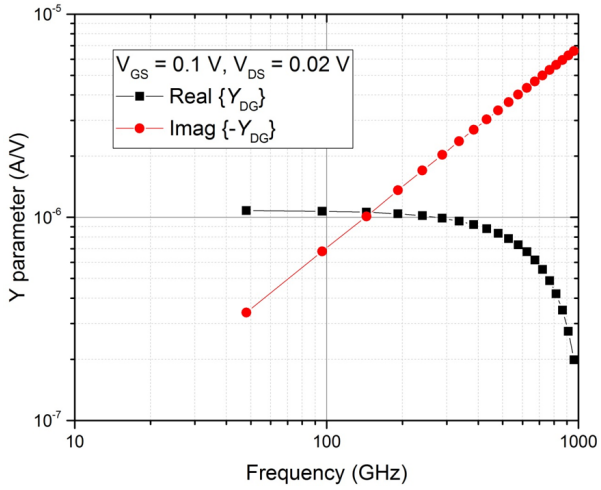

Fig. 9. $Y_{DG}(\omega)$ of the nanosheet transistor. The frequency varies from 48 GHz to 1 THz. V_{GS} = 0.1 V and V_{DS} = 0.02 V. The wideband limit approximation is applied.

References

[1] S. Datta, "A simple kinetic equation for steady-state quantum transport," *Journal of Physics: Condensed Matter*, vol. 2, no. 40, pp. 8023–8052, oct 1990.

[2] ——, "Nanoscale device modeling: the greenâs function method," *Superlattices and microstructures*, vol. 28, no. 4, pp. 253–278, 2000.

[3] ——, *Quantum Transport: Atom to Transistor*. Cambridge University Press, 2005.

[4] S. Tiwari, M. V. Fischetti, and S. E. Laux, "Overshoot in transient and steady-state in GaAs, InP, Ga.47In.53As and InAs bipolar transistors," in *1990 International Electron Device Meeting*, 1990, pp. 435–438, doi: 10.1109/IEDM.1990.237 074.

[5] S. E. Laux and M. V. Fischetti, "Monte Carlo study of velocity overshoot in switching a 0.1-micron CMOS inverter," in *1997 International Electron Device Meeting*, 1997, pp. 877–890, doi: 10.1109/IEDM.1997.650 521.

[6] Y. Koseki, V. Rhzhii, T. Otsuji, V. V. Popov, and A. Satou, "Giant plasmon instability in a dual-grating-gate graphene field-effect transistor," *Physical Review B*, vol. 93, no. 24, p. 245408, June 2016, doi: 10.1103/PhysRevB.93.245408.

[7] S. Di, K. Zhao, T. Lu, G. Du, and X. Liu, "Investigation of transient responses of nanoscale transistors by deterministic solution of the time-dependent BTE," *Journal of Computational Electronics*, vol. 15, no. 3, pp. 770–777, September 2016, doi: 10.1007/s10825-016-0818-1.

[8] Y. Wei and J. Wang, "Current conserving nonequilibrium ac transport theory," *Phys. Rev. B*, vol. 79, p. 195315, May 2009. [Online]. Available: https://link.aps.org/doi/10.1103/PhysRevB.79.195315

[9] O. Shevtsov and X. Waintal, "Numerical toolkit for electronic quantum transport at finite frequency," *Phys. Rev. B*, vol. 87, p. 085304, Feb 2013. [Online]. Available: https://link.aps.org/doi/10.1103/PhysRevB.87.085304

[10] M. J. McLennan, Y. Lee, and S. Datta, "Voltage drop in mesoscopic systems: A numerical study using a quantum kinetic equation," *Phys. Rev. B*, vol. 43, pp. 13 846–13 884, Jun 1991. [Online]. Available: https://link.aps.org/doi/10.1103/PhysRevB.43.13846

[11] S.-M. Hong and J.-H. Jang, "Numerical simulation of plasma oscillation in 2-D electron gas using a periodic steady-state solver," *IEEE Transactions on Electron Devices*, vol. 62, no. 12, pp. 4192–4198, Dec 2015, 10.1109/TED.2015.2489220.

[12] ——, "Transient simulation of semiconductor devices using a deterministic Boltzmann equation solver," *IEEE Journal of the Electron Devices Society*, vol. 6, pp. 156–163, 2018, doi: 0.1109/JEDS.2017.2780837.